Molecular Rotor Inside a Phosphonate Cavitand: Role of Supramolecular Interactions

2 AUTHORS:

Deepthi Jose

Ecole Centrale de Lyon

14 PUBLICATIONS **282** CITATIONS

SEE PROFILE

Ayan Datta

Indian Association for the Cultivation of Scie…

96 PUBLICATIONS **1,490** CITATIONS

SEE PROFILE

Molecular Rotor Inside a Phosphonate Cavitand: Role of Supramolecular Interactions

Deepthi Jose and Ayan Datta*

School of Chemistry, Indian Institute of Science Education and Research Thiruvananthapuram, CET Campus, Thiruvananthapuram- 695016, Kerala, India

ABSTRACT A supramolecular rotor is designed based on a phosphonate cavitand$\cdots$methanol/ethanol complex. Density functional theory (DFT) calculations reveal a very small barrier for rotation of methanol inside the cavity. The origin for such almost barrierless rotation is traced to the low-energy cost associated with breaking the weak O−H$\cdots$O interactions in the ground-state complex and substantial stabilization of the transition state (TS) due to C−H$\cdots\pi$ interactions. Available crystal structures of the complexes are indicative of such supramolecular rotation. Further experimental signatures are predicted through NMR calculations to detect such rotations at liquid N_2 temperature.

SECTION Dynamics, Clusters, Excited States
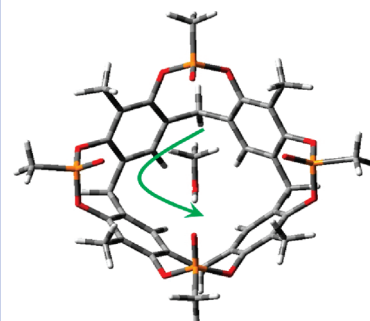
The past decade has witnessed a major development of materials at the molecular scale that have exotic electronic, optical and mechanical properties.[1−3] Among these, molecular machines are probably the most interesting because of their immediate application in cellular drug delivery and artificial nanomechanical shuttles that mimic biological functions.[4−7] Many of these newly synthesized molecules utilized restricted rotation along bonds through rational control of the steric interactions for barrier crossing.[8−12] Another popular strategy is to design molecular units that undergo conformation changes upon being oxidized/reduced or photoexcitation, thereby representing ON and OFF states under controllable conditions.[13,14] Atomic force micriscopy (AFM) and scanning tunneling microscopy (STM) studies can precisely image the physical motion in such molecular components on surfaces. Along with such progress, the design of many supramolecular complexes from simple molecular units through tailored weak intermolecular forces such as H-bonding, π-stacking, and cation−π interactions is quite promising.[15,16] However, a proper utilization of such weak intermolecular forces for a rational design of molecular motors is yet to be achieved. In this communication, we have designed an inclusion complex of methanol/ethanol (Figure 1, top panel) that acts as a molecular rotor inside a phosphonate cavitand with a small barrier height for rotation. The crystal structure of the inclusion complex shows a clear signature of the rotating behavior of methanol inside the cavity. We also propose strategies to control the rate of rotation of the molecules inside such cavities by substituting bulky groups that increase the barrier for rotation.

Geometry optimization was performed on the inclusion complexes at the MPW1K/6-31+G(d,p) level.[17] Selection of a density functional theory (DFT) functional that accurately describes the rotation along small barrier heights is a difficult problem. The choice of the MPW1K functional for the cavi-

tand$\cdots$molecule interaction is based on the fact that, for ethanol, MPW1K/6-31+G(d,p) calculations correctly predict the anticonformer as the stable species (by 36 cm^{-1}) compared to the gauche form (experimental energy difference between the two conformers is 39.2 cm^{-1}),[18] while the popular B3LYP/6-31+G(d,p) level predicts the gauche form as the lowest energy conformer. All the calculations reported have been performed using the Gaussian 03 suite of programs.[19] Several low-energy orientations/symmetries were considered (for **I−VIII**) and the lowest energy structures are reported in Figure 1 (bottom panel, all of them have C_s symmetries). Additional frequency calculations verified the absence of any vibrational instability in ground-state structures. The transition states for methanol/ethanol rotation are verified by an imaginary vibrational mode corresponding to molecular rotation within the cavity. The binding energies for methanol with the cavitand with various side groups is $\sim$3 kcal/mol higher than for ethanol, suggesting that the available free volume inside the cavity is more accommodative to the smaller molecule. This is also understood from the higher barrier height to the rotation of ethanol, suggesting a more constrained environment.
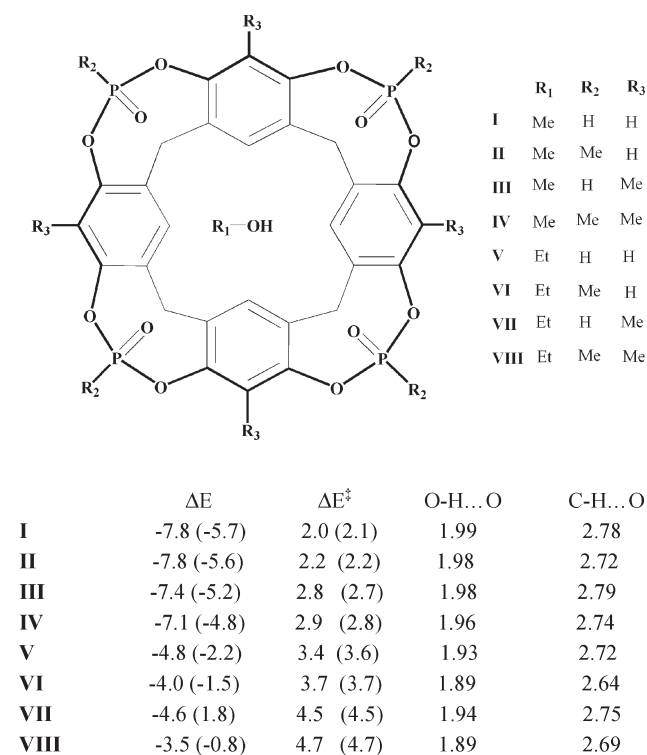
The crystal structure for the methanol$\cdots$phosphonate cavitand has been elucidated by Dalcanale and co-workers.[20] In Figure 2A, the structure of the inclusion complex **(IV)** as retrieved from the crystal is shown. The fluxional behavior of the methyl group as well as the −OH group is seen in the crystal with multiple possible positions for the hydrogens on the oxygen atom and the carbon atom. Such disorder in the crystal structure typically arises as a result of rapid internal

rotation in molecules. The basis set superposition error (BSSE)-corrected[21] (uncorrected) binding energy of **IV** is -4.8 kcal/mol (-7.1 kcal/mol). The stability for this structure (Figure 2B) as well as the other inclusion complexes is understood on the basis of one strong $O-H\cdots O$ hydrogen bond ($H\cdots O$ contact = 1.96 Å: HB1) and three weak $C-H\cdots O$ hydrogen bonds ($H\cdots O$ contact = 2.74 Å: HB2 and HB3; $H\cdots O$ contact = 2.91 Å: HB4). The $O-H\cdots O$ H-bond for the molecule$\cdots$cavity in **IV** has an $\angle O-H\cdots O$ of 160.5 degrees

		R_1	R_2	R_3
I		Me	H	H
II		Me	Me	H
III		Me	H	Me
IV		Me	Me	Me
V		Et	H	H
VI		Et	Me	H
VII		Et	H	Me
VIII		Et	Me	Me

|	ΔE	$\Delta E^{\ddagger}$	$O-H\ldots O$	$C-H\ldots O$
I	-7.8 (-5.7)	2.0 (2.1)	1.99	2.78
II	-7.8 (-5.6)	2.2 (2.2)	1.98	2.72
III	-7.4 (-5.2)	2.8 (2.7)	1.98	2.79
IV	-7.1 (-4.8)	2.9 (2.8)	1.96	2.74
V	-4.8 (-2.2)	3.4 (3.6)	1.93	2.72
VI	-4.0 (-1.5)	3.7 (3.7)	1.89	2.64
VII	-4.6 (1.8)	4.5 (4.5)	1.94	2.75
VIII	-3.5 (-0.8)	4.7 (4.7)	1.89	2.69

Figure 1. (Top panel) Structures of the cavitand$\cdots$methanol/ethanol complexes. (Bottom panel) Binding energies (ΔE, in kcal/mol; BSSE corrected within bracket), barrier heights for rotation ($\Delta E^{\ddagger}$ in kcal/mol; BSSE corrected within bracket), $O-H\cdots O$ distances (in Å), and $C-H\cdots O$ distances (in Å).

and a zero dihedral angle between the $C-O$ axis of methanol and the $P=O$ axis of the phosphate. This interaction can be well classified within the realms of a traditional $O-H\cdots O$ bond (bond energy ~ 5 kcal/mol, $\angle O-H\cdots O \sim 135-180$ degrees and $H\cdots O$ contact distance ~ 2.0 Å).[9] The ability of the hydrogen bonds to sustain themselves in the ground state is understood by tracking the zero-point energy (ZPE) vibrational mode (unscaled) of 30.9 cm^{-1}, which disrupts the $O-H\cdots O$ hydrogen bond. This is much smaller than both the binding energy as well as the barrier height of the potential energy surface (PES) for rotation of methanol inside the cavity, suggesting that H-bonds are stable and not transient.[22]

The PES for rotation of the molecule inside the cavitand was calculated by scanning the movement of the $-OH$ group between the four $P=O$ groups. Because of the overall C_2 symmetry of the cavitand, the scan for rotation for φ [defined by $H_3C-O-H\cdots O1$ (phosphate)] = $0-90°$ (1/4 of the quadrant, between two nearest neighbor $P=O$) is sufficient. Rotation of the methanol between the two $P=O$ leads to a transition state with the $-OH$ of the methanol pointing toward the $H/-C-H$ of the $H/-CH_3$ group on the aromatic ring at $\varphi = 45°$ (see Supporting Information). The internal energy ($\Delta E^{\ddagger}$), enthalpy ($\Delta H^{\ddagger}$), and free energy ($\Delta G^{\ddagger}$) barriers for this rotation in **IV** and **VIII** are 2.9 and 4.7 kcal/mol, 1.2 and 3.6 kcal/mol, and 2.8 and 3.7 kcal/mol, respectively (see Figure 3A). The origin of the low barrier can be attributed to mainly two effects. First, unlike rotation across bonds that causes orbital symmetry breaking, rotation of these molecules involves cleavage of only weak intermolecular interactions. Second, even the transition states are stabilized through additional $C-H\cdots\pi$ interactions of the alkyl group with the aromatic rings. In **IV**, one of the $C-H$ bonds of the methyl group (opposite to the $C-O$ bond) has a short contact $C-H\cdots\pi$ distance of 2.74 Å from the center of the aromatic ring. A small barrier height for rotation of methanol within the cavity suggests perpetual motion of the guest inside the host. The transition-state theory (TST)[23] predicts a rapid rate of methanol rotation (k) $\sim 5.7 \times 10^{10}$ s^{-1} at room temperature.

(A)   **(B)**
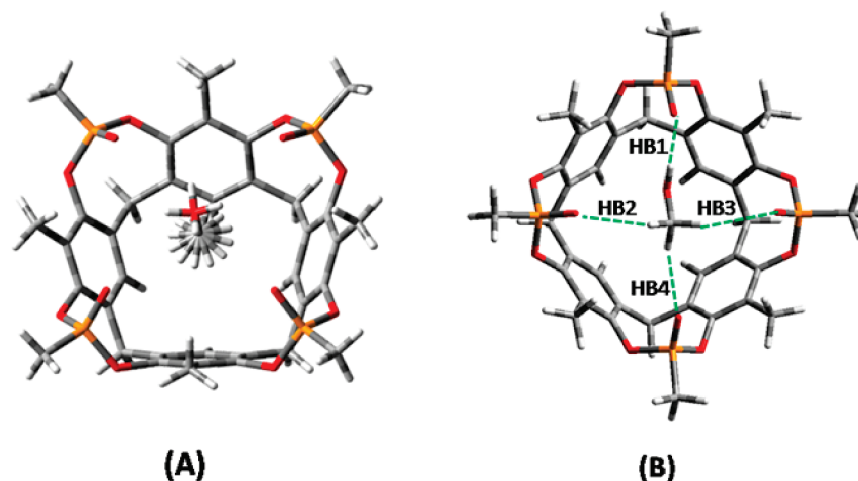
Figure 2. (A) Structure of the inclusion complex as retrieved from crystal. (B) Geometry-optimized structure of the inclusion complex.
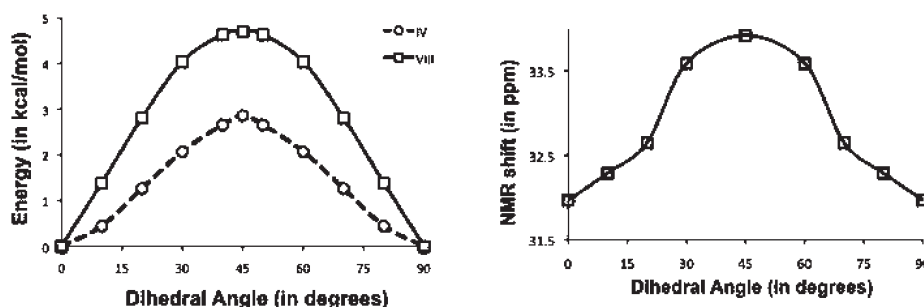
Figure 3. (A) Potential energy profile for rotation of the methanol and ethanol in **IV** and **VIII**, respectively. (B) NMR intensity for the H-atom of the −OH in methanol along the same dihedral angle, φ in **IV**.

It is possible to experimentally verify such rapid movement of the molecule within the cavity through NMR at low temperatures (TST predicts $k \sim 1.6 \times 10^4 \text{ s}^{-1}$ at 77 K in **IV**). We have performed ^{1}H NMR calculations (using the GIAO method[24] at the MPW1K/6-31+G(d,p) level) on the complex in **IV**. There are four distinct shifts associated with the four types of protons, namely, (a) the methanol −OH proton, (b) the proton from the methyl group in methanol, (c) the proton from the methyl group in the phosphonate cavitand, and the (d) aromatic proton on the rings. For the equilibrium structure of the complex, the shifts (in ppm) are 31.97, 29.86, 30.27, and 29.64 for a, b, c, and d, respectively. The maximum shift occurs for "a" in the −OH group. For the fully formed $CH_3-OH\cdots O = P$ hydrogen bond ($\varphi = 0$ and 90°), the methanol proton is most deshielded due to the presence of the two highly electronegative O atoms in close proximity. Rotation of methanol from the H-bonded complex reduces deshielding, and a maximum shift is observed for $\varphi = 45°$, corresponding to the transition state for rotation (Figure 3). A temperature-dependent NMR for the cavitand···molecule complex can thus provide signatures of molecular rotor behavior. The presence of a more bulky side group in alcohol reduces the rate of molecular rotation, and such motion should be easily detectable. The presence of four −P=O groups pointing toward the cavity act as pawl, while the alcohol acts as a ratchet. However, the symmetry of the complex ensures equally probable motion in clockwise and counter-clockwise directions. Nevertheless, by suitable synthesis of a cavity with steric asymmetry through selective removal of one phosphate group out of the four, the molecular motion can be made unidirectional, and the motion might be tracked at low temperatures. We look forward to an experimental test of our computational predictions.

SUPPORTING INFORMATION AVAILABLE Cartesian coordinates, energies, and harmonic frequencies for **I**−**VIII** and complete reference 19. This material is available free of charge via the Internet at http://pubs.acs.org.

AUTHOR INFORMATION

Corresponding Author:

*To whom correspondence should be addressed. E-mail: ayan@iisertvm.ac.in.

REFERENCES

(1) Ball, P. *Designing the Molecular World*; Princeton University Press: Princeton, NJ, 1994.

(2) *Photophysics of Molecular Materials*; Lanzani, G., Ed.; Wiley-VCH: Weinheim, Germany, 2006.

(3) *Molecular Motors*; Schliwa, M., Ed.; Wiley-VCH: Weinheim, Germany, 2004.

(4) Kay, E. R.; Leigh, D. A.; Zerbetto, F. Synthetic Molecular Motors and Mechanical Machines. *Angew. Chem., Int. Ed.* **2007**, *46*, 72–191.

(5) Michl, J.; Sykes, C. H. Molecular Rotors and Motors: Recent Advances and Future Challenges. *ACS Nano* **2009**, *3*, 1042–1048.

(6) Kottas, G. S.; Clarke, L. I.; Horinek, D.; Michl, J. Artificial Molecular Rotors. *Chem. Rev.* **2005**, *105*, 1281–1376.

(7) Ballardini, R.; Balzani, V.; Credi, A.; Gandolfi, M. T.; Venturi, M. Artificial Molecular-Level Machines: Which Energy to Make them Work? *Acc. Chem. Res.* 2001, *34*, 445−455.

(8) Feringa, B. L. In Control of Motion: From Molecular Switches to Molecular Motors. *Acc. Chem. Res.* **2001**, *34*, 504–513.

(9) Geertsema, E. M.; van der Molen, S. J.; Martens, M.; Feringa, B. L. Optimizing Rotary Processes in Synthetic Molecular Motors. *Proc. Natl. Acad. Sci. U.S.A.* **2009**, *106*, 16919–16924.

(10) Dominguez, Z.; Khuong, T-A. V.; Dang, H.; Sanrame, C. N.; Nunez, J. E.; Garcia-Garibay, M. A. Molecular Compasses and Gyroscopes with Polar Rotors: Synthesis and Characterization of Crystalline Forms. *J. Am. Chem. Soc.* **2003**, *125*, 8827–8837.

(11) Torras, J.; R-Ropero, F.; Bertran, O.; Aleman, C. Controlled Isomerization of a Light-Driven Molecular Motor: A Theoretical Study. *J. Phys. Chem. C* **2009**, *113*, 3574–3580.

(12) Hrovat, D. A.; Borden, W. T.; Eaton, P. E.; Kahr, B. A Computational Study of the Interactions among the Nitro Groups in Octanitrocubane. *J. Am. Chem. Soc.* **2001**, *123*, 1289–1293.

(13) Kanazawa, H.; Higuchi, M.; Yamamoto, K. An Electric Cyclophane: Cavity Control Based on the Rotation of a Paraphenylene by Redox Switching. *J. Am. Chem. Soc.* **2005**, *127*, 16404–16405.

(14) Brough, B.; Northrop, B. H.; Schmidt, J. J.; Tseng, H.-R.; Houk, K. N.; Stoddart, J. F.; Ho, C.-M. Evaluation of Synthetic Linear Motor-Molecule Actuation Energetics. *Proc. Natl. Acad. Sci. U.S.A.* **2006**, *103*, 8583–8588.

(15) *The Weak Hydrogen Bond: In Structural Chemistry and Biology*; Desiraju, G. R.; Steiner, T., Eds.; Oxford University Press: Oxford, U.K., 1999.

(16) Datta, A.; Pati, S. K. Dipolar Interactions and Hydrogen Bonding in Supramolecular Aggregates: Understanding Cooperative Phenomena for 1st Hyperpolarizability. *Chem. Soc. Rev.* **2006**, *35*, 1305–1323.

(17) Lynch, B. J.; Fast, P. L.; Harris, M.; Truhlar, D. G. Adiabatic Connection for Kinetics. *J. Phys. Chem. A* **2000,** *104*, 4811–4815.

(18) Ning, C. G.; Luo, Z. H.; Huang, Y. R.; Hajgato, B.; Morini, F.; Liu, K.; Zhang, S. F.; Deng, J. K.; Deleuze, M. S. Investigation of the Molecular Conformations of Ethanol Using Electron Momentum Spectroscopy. *J. Phys. B: At. Mol. Opt. Phys.* **2008,** *41*, 175103–175113.

(19) Frisch, M. J.; Trucks, G. W.; Schlegel, H. B.; Scuseria, G. E.; Robb, M. A.; Cheeseman, J .R.; Montgomery, J. A.; Vreven, Jr. T.; Kudin, K. N.; Burant, J. C.; et al. *Gaussian 03*; Gaussian, Inc.: Wallingford, CT, 2003.

(20) Melegari, M.; Suman, M.; Pirondini, L.; Moiani, D.; Massera, C.; Ugozzoli, F.; Kalenius, E.; Vainiotalo, P.; Mulatier, J.-C.; Dutasta, J.-P.; Dalcanale, E. Supramolecular Sensing with Phosphonate Cavitands. *Chem.—Eur. J.* **2008,** *14*, 5772–5779.

(21) Boys, S. F.; Bernardi, F. The Calculation of Small Molecular Interactions by the Differences of Separate Total Energies. Some Procedures with Reduced Errors. *Mol. Phys.* **1970,** *19*, 553–566.

(22) Goswami, M.; Arunan, E. The Hydrogen Bond: A Molecular Beam Spectroscopist's View with a Universal Appeal. *Phys. Chem. Chem. Phys.* **2009,** *11*, 8974–8983.

(23) *Chemical Kinetics*, 3rd ed.; Laidler, K. J., Ed.; Prentice Hall: New Jersey, 1987.

(24) Schleyer, P. v. R.; Maerker, C.; Dransfeld, A.; Jiao, H.; Eikema-Hommas, N. J. R. v. Nucleus-Independent Chemical Shifts: A Simple and Efficient Aromaticity Probe. *J. Am. Chem. Soc.* **1996,** *118*, 6317–6318.